



Cite this: DOI: 10.1039/c9dt01103j

# Carbonate encapsulation from dissolved atmospheric CO<sub>2</sub> into a polyoxovanadate capsule†‡

Sateesh Mulkapuri,  Sathish Kumar Kurapati  and Samar K. Das \*

An aqueous synthesis, involving the reduction of the VO<sub>3</sub><sup>−</sup> anion in a mild alkaline pH in the presence of α-Bi<sub>2</sub>O<sub>3</sub>, led to the formation of a fully reduced polyoxovanadate (POV) capsule, with CO<sub>3</sub><sup>2−</sup> anion encapsulation in its internal cavity, in the compound [Na<sub>6</sub>(H<sub>2</sub>O)<sub>24</sub>][H<sub>8</sub>V<sub>15</sub><sup>IV</sup>O<sub>36</sub>(CO<sub>3</sub>)·3N<sub>2</sub>H<sub>4</sub>·10H<sub>2</sub>O (**1**). This CO<sub>3</sub><sup>2−</sup> anion encapsulation, the source of which is absorbed aerial CO<sub>2</sub> in the pertinent aqueous alkaline reaction mixture, occurs only in the presence of α-Bi<sub>2</sub>O<sub>3</sub>. Compound **1** crystals, upon exposure to HCl acid vapor, exclude CO<sub>2</sub> gas that can react with the Grignard reagent (PhMgBr) to form triphenylcarbinol and benzoic acid; during this solid–vapor interface reaction, compound **1** itself transforms into an amorphous material that includes the Cl<sup>−</sup> anion but could not be characterized unambiguously. Thus, we have synthesized a chloride ion (Cl<sup>−</sup>) encapsulated compound [Na<sub>10</sub>(H<sub>2</sub>O)<sub>24</sub>][H<sub>3</sub>V<sub>15</sub><sup>IV</sup>O<sub>36</sub>(Cl)]·6H<sub>2</sub>O (**2**) in a direct synthesis protocol, which has been characterized by crystallography as well as by other spectroscopic methods. Compounds **1** and **2**, each having fifteen vanadium(IV) centers, exhibit interesting magnetism in their solid states. The temperature-dependent magnetic susceptibilities for compounds **1** and **2** have been recorded at 0.1 T in the temperature range of 3–300 K. The temperature-dependent magnetic susceptibilities of compounds **1** and **2** are shown in the form of χ<sub>M</sub> vs. *T* and their product χ<sub>M</sub>*T* vs. *T* plots.

Received 13th March 2019,  
Accepted 5th May 2019

DOI: 10.1039/c9dt01103j

rsc.li/dalton

## Introduction

Polyoxometalates (POMs), the all-inorganic metal–oxygen cluster species having wide structural diversity<sup>1–14</sup> (in size as well as in shape) and diverse applications (in catalysis,<sup>4,5</sup> photochemistry,<sup>5</sup> electrochemistry,<sup>4–11</sup> medicine,<sup>12</sup> magnetism,<sup>13–20</sup> proton conduction,<sup>21</sup> etc.), exhibit interesting host–guest chemistry.<sup>21–29</sup> Complete encapsulation of a guest molecule/ion in the internal cavity of the host POM cluster is of considerable interest because it represents a unique supra-molecular core–shell entity, in which the guest species influences the electronic properties of the resulting host–guest system.<sup>21–49</sup> In this regard, among POMs, polyoxovanadates (POVs) draw special attention, because a number of POVs are

known to have well-defined internal cavities for encapsulation.<sup>22–25</sup> All these shell-containing POV clusters, capable of encapsulating a guest species, have a common feature of the presence of a square-pyramidal {O<sub>4</sub>V=O} polyhedron, which is believed to have a tendency to form the cage or shell.<sup>23–27,30–49</sup> The presence of the guest species, such as halide, pseudohalide, inorganic, or organic anions in the concerned synthesis reaction mixture, plays a key role in the isolation of the resulting host–guest compounds. The guest-anionic-species like Cl<sup>−</sup>, Br<sup>−</sup>, I<sup>−</sup>, CN<sup>−</sup>, CO<sub>3</sub><sup>2−</sup>, NO<sup>−</sup>, NO<sub>2</sub><sup>−</sup>, N<sub>3</sub><sup>−</sup>, PO<sub>4</sub><sup>3−</sup>, HCOO<sup>−</sup>, CH<sub>3</sub>COO<sup>−</sup>, SH<sup>−</sup>, SCN<sup>−</sup>, SO<sub>3</sub><sup>2−</sup>, SO<sub>4</sub><sup>2−</sup>, ClO<sub>4</sub><sup>−</sup> are known to be encapsulated by the following shell-containing POV hosts: [V<sub>12</sub>O<sub>32</sub>(X)]<sup>5−</sup> (X = NO<sup>−</sup>, CN<sup>−</sup>, OCN<sup>−</sup>, NO<sub>2</sub><sup>−</sup>, NO<sub>3</sub><sup>−</sup>, HCO<sub>2</sub><sup>−</sup>, CH<sub>3</sub>COO<sup>−</sup>, Cl<sup>−</sup>, Br<sup>−</sup>, I<sup>−</sup>);<sup>31–34</sup> [V<sub>12</sub>O<sub>32</sub>(X)]<sup>4−</sup> (X = CO<sub>2</sub>, CH<sub>3</sub>CN, DCM, CH<sub>3</sub>NO<sub>2</sub>, CH<sub>3</sub>Br);<sup>26,30</sup> [V<sub>15</sub>O<sub>36</sub>(CO<sub>3</sub>)]<sup>7−</sup>;<sup>24,25</sup> [V<sub>15</sub>O<sub>36</sub>(X)]<sup>6−</sup> (X = Cl<sup>−</sup>, Br<sup>−</sup>, I<sup>−</sup>);<sup>35,36</sup> [V<sub>16</sub>O<sub>38</sub>(X)]<sup>*n*−</sup> (X = F<sup>−</sup>, Cl<sup>−</sup>, Br<sup>−</sup>, CN<sup>−</sup>, H<sub>2</sub>O; *n* = 3, 4);<sup>37–45</sup> [V<sub>16</sub>O<sub>39</sub>(Cl)]<sup>6−</sup>;<sup>45</sup> [V<sub>16</sub>O<sub>42</sub>(Cl)]<sup>8−</sup>;<sup>42</sup> [V<sub>18</sub>O<sub>42</sub>(X)]<sup>*n*−</sup> and [V<sub>18</sub>O<sub>44</sub>(X)]<sup>*n*−</sup> (X = H<sub>2</sub>O, Cl<sup>−</sup>, Br<sup>−</sup>, I<sup>−</sup>, SO<sub>4</sub><sup>2−</sup>, SO<sub>3</sub><sup>2−</sup>, VO<sub>4</sub><sup>3−</sup>, N<sub>3</sub><sup>−</sup>, NO<sub>2</sub><sup>−</sup>, NO<sub>3</sub><sup>−</sup>, SH<sup>−</sup>, HCOO<sup>−</sup>; *n* = 5–15);<sup>46–49</sup> [V<sub>22</sub>O<sub>54</sub>(X)]<sup>7−</sup> (X = ClO<sub>4</sub><sup>−</sup>, N<sub>3</sub><sup>−</sup>); [V<sub>30</sub>O<sub>74</sub>{(V<sub>4</sub>O<sub>4</sub>)O<sub>4</sub>}]<sup>10−</sup>.<sup>46</sup> Thus, chloride anion (Cl<sup>−</sup>) encapsulation was found in diverse cage-containing POV systems, as reported by Müller,<sup>35</sup> Peng,<sup>37</sup> Khan,<sup>42</sup> Hayashi<sup>43</sup> and their co-workers. Among these host–guest systems, carbonate anion (CO<sub>3</sub><sup>2−</sup>) encapsulation by the mixed-valence POV cluster anion [V<sub>7</sub>V<sub>8</sub><sup>IV</sup>O<sub>36</sub>(CO<sub>3</sub>)]<sup>7−</sup> has drawn

School of Chemistry, University of Hyderabad, P.O. Central University, Hyderabad – 500046, India. E-mail: skdas@uohyd.ac.in, samar439@gmail.com; Fax: +91-40-2301-2460; Tel: +91-40-2313-4853

† We would like dedicate this article to Prof. V. Chandrasekhar on the occasion of his 60<sup>th</sup> birthday.

‡ Electronic supplementary information (ESI) available: Bond distances and bond angles tables, PXRD patterns, TGA-DTA, TGA-IR, TGA-Mass, BVS calculations, carbonate ion confirmation tests, volumetric redox titrations for vanadium centers and reports of elemental analysis. CCDC 1839257 (2). For ESI and crystallographic data in CIF or other electronic format see DOI: 10.1039/c9dt01103j

our special attention, because the  $\text{CO}_3^{2-}$  anion can be derived from  $\text{CO}_2$  gas ( $\text{CO}_2 + \text{OH}^- \rightarrow \text{CO}_3^{2-} + \text{H}^+$ ), which is an important component in our earth-surface atmosphere in the context of global warming.<sup>50,51</sup> Müller and coworkers reported the first mixed-valent POV encapsulated carbonate compound  $\text{Li}_7[\text{V}_7^{\text{V}}\text{V}_8^{\text{IV}}\text{O}_{36}(\text{CO}_3)] \sim \text{ca.} \cdot 39\text{H}_2\text{O}$  in 1990, which was synthesized in the presence of  $\text{Li}_2\text{CO}_3$ .<sup>24</sup> Four years later, Yamase and Ohtaka prepared the same mixed-valent host-guest compound  $\text{K}_5\text{H}_2[\text{V}_7^{\text{V}}\text{V}_8^{\text{IV}}\text{O}_{36}(\text{CO}_3)] \cdot 14.5\text{H}_2\text{O}$  (but with different cations), which was synthesized by photolyzing an aqueous  $\text{CH}_3\text{OH}$  solution mixture of  $[\text{V}_4\text{O}_{12}]^{4-}$  in the presence of  $\text{K}_2\text{CO}_3$ .<sup>25</sup> There are reports on the interactions between  $\text{CO}_2$  and POMs.<sup>52–57</sup>

Herein, we report a unique aqueous synthesis of a POM-based host-guest system  $[\text{Na}_6(\text{H}_2\text{O})_{24}][\text{H}_8\text{V}_{15}^{\text{IV}}\text{O}_{36}(\text{CO}_3)] \cdot 3\text{N}_2\text{H}_4 \cdot 10\text{H}_2\text{O}$  (**1**), in which the fully reduced POV capsule captures dissolved aerial  $\text{CO}_2$  from an alkaline aqueous synthesis mixture in the form of carbonate anion. The absorption of aerial  $\text{CO}_2$  by an aqueous alkaline solution is not surprising. But, the fact that the encapsulation of this dissolved aerial  $\text{CO}_2$  into the internal cavity of the POV capsule does not happen 'just like that' without the presence of some amount of  $\alpha\text{-Bi}_2\text{O}_3$  in the concerned reaction mixture, is surprising. We could isolate compound **1** from an aqueous alkaline solution of sodium vanadate under reducing condition, only in the presence of  $\alpha\text{-Bi}_2\text{O}_3$ . The compound  $[\text{Na}_6(\text{H}_2\text{O})_{24}][\text{H}_8\text{V}_{15}^{\text{IV}}\text{O}_{36}(\text{CO}_3)] \cdot 3\text{N}_2\text{H}_4 \cdot 10\text{H}_2\text{O}$  (**1**), upon exposure to  $\text{HCl}$  vapor, excluded carbonate in the form of  $\text{CO}_2$ , whereby compound **1** transformed into an amorphous substance, which could not be characterized unambiguously, but was found to contain chlorine (from elemental analysis). We, therefore, synthesized a chloride-included compound  $[\text{Na}_{10}(\text{H}_2\text{O})_{24}][\text{H}_3\text{V}_{15}^{\text{IV}}\text{O}_{36}(\text{Cl})] \cdot 6\text{H}_2\text{O}$  (**2**), in which the same POV cluster capsule, as found in compound **1**, encapsulates chloride anion in its cavity, as observed from its crystal structure determination.

## Experimental

All the chemicals were of analytical grade and used as received. Deionised water was used for all the experiments. Compounds **1** and **2** were synthesized by conventional wet synthesis methods under ambient atmosphere.

### Physical measurements

Elemental analysis was performed using a FLASH EA series 1112 CHNS analyser. A Bruker Tensor II equipped with Platinum ATR (Attenuated Total Reflectance) accessory was used to collect the FT-IR spectra. A TA instrument Q600 TG/DTA coupled with a Bruker Tensor II ATR-IR was used to record TGA-FTIR measurements. TG analyses were carried out on a PerkinElmer – STA 6000, and TG-Mass analyses were performed on a PerkinElmer – STA 6000 coupled with a PerkinElmer – Clarus SQ8S mass spectrometer. Raman spectra were recorded on a Wi-Tec alpha 300AR laser confocal optical microscope (T-LCM) facility equipped with a Peltier-cooled CCD detector using a 785 nm Argon ion laser. Magnetic sus-

ceptibilities were measured in the temperature range of 3–300 K on a Quantum Design VSM SQUID. ICP-OES elemental analyses were performed on an ICP-OES Varian 720ES. XPS analyses of the powdered samples were performed on an Omicron Nanotech ESCA<sup>+</sup> (Oxford Instruments, Germany). Powder X-ray diffraction (PXRD) patterns of **1** and **2** were recorded on a Bruker D8-Advance diffractometer using graphite monochromated  $\text{Cu K}\alpha 1$  (1.5406 Å) and  $\text{K}\alpha 2$  (1.54439 Å) radiation.

### Synthesis of the compound

#### $[\text{Na}_6(\text{H}_2\text{O})_{24}][\text{H}_8\text{V}_{15}^{\text{IV}}\text{O}_{36}(\text{CO}_3)] \cdot 3\text{N}_2\text{H}_4 \cdot 10\text{H}_2\text{O}$ (**1**)

3.66 g of  $\text{NaVO}_3$  was added to 100 mL of hot water (temp. 85–90 °C) in a 250 mL conical flask to give a clear colourless solution. 0.31 g of solid  $\alpha\text{-Bi}_2\text{O}_3$  and 0.72 g of solid  $\text{NaOH}$  were added subsequently to the above solution and immediately covered with a watch glass and stirred for 30 min on a hot plate (temp. 85–90 °C). Afterwards, 2.5 g of  $\text{N}_2\text{H}_5 \cdot \text{HSO}_4$  was added in small portions (to avoid aggressive effervescence) to the above reaction mixture. After the addition of  $\text{N}_2\text{H}_5 \cdot \text{HSO}_4$ , the colour of the solution changed from yellow to dark green, and this was stirred for another 15 min and cooled to room temperature. The solution was filtered, and the filtrate was left undisturbed for 24 hours in an open atmosphere. The dark brown coloured precipitate formed, was filtered off and the dark green coloured filtrate was kept undisturbed for crystallization. After 10 days, the dark green crystals along with a minute amount of unidentified precipitate settled and were filtered, washed three times with a small amount of ice-cold water (~20 mL), washed twice with 20 mL of an ethanol and ice-cold water mixture (1 : 1 ratio) and dried in air at room temperature. Yield: 2.21 g (50% based on vanadium). Anal. calcd % for  $\text{V}_{15}\text{Na}_6\text{O}_{79}\text{C}_1\text{H}_{88}$ : V, 33.81; Na, 6.09; C, 0.55; H, 3.61, N, 3.76. Found: V, 34.96 (ICP-OES); Na, 6.58 (ICP-OES); C, 0.61 (CHN); H, 3.98; (CHN); N, 3.72; (CHN).

#### $[\text{Na}_{10}(\text{H}_2\text{O})_{24}][\text{H}_3\text{V}_{15}^{\text{IV}}\text{O}_{36}(\text{Cl})] \cdot 6\text{H}_2\text{O}$ (**2**)

3.66 g of  $\text{NaVO}_3$  was added to 100 mL of hot water (temp. 85–90 °C) in a 250 mL conical flask to give a colourless solution. 0.31 g of solid  $\alpha\text{-Bi}_2\text{O}_3$  and 0.72 g of solid  $\text{NaOH}$  were added subsequently to the above solution and immediately covered with a watch glass and stirred for 30 min on a hot plate (temp. 85–90 °C). 2.5 g of  $\text{N}_2\text{H}_5 \cdot \text{HSO}_4$  was added in small portions (to avoid effervescence) to the resulting reaction mixture. After the addition of  $\text{N}_2\text{H}_5 \cdot \text{HSO}_4$ , the colour of the solution changed from yellow to dark green, and this was stirred for another 15 min. 4.5 g of solid  $\text{NaCl}$  was added to the reaction mixture, and the stirring was continued for 10 more minutes. The reaction contents were cooled to room temperature, and the solution was filtered. The filtrate was kept undisturbed in an open atmosphere; after 4 days, black-colored crystals along with a minute amount of unidentified precipitate were obtained, filtered, washed three times with a minimum amount of ice-cold water (~20 mL), washed twice with 20 mL of an ethanol and ice-cold water mixture (1 : 1 ratio) and dried in air at room temperature. Yield: 2.35 g

(55.5% based on vanadium from the product). Anal. calcd % for  $V_{15}Na_{10}O_{66}ClH_{63}$ : V, 35.56; Na, 10.70; Cl, 1.65. Found: V, 35.53 (ICP-OES); Na, 10.58 (ICP-OES); Cl, 1.68 (ICP-OES).

### Carbonate ion confirmation test

**Test 1.** 0.1 M calcium hydroxide solution was added dropwise to (0.1 mmol) 5 mL of the solution of compound **1** (deep green solution). Cloudy white precipitation slowly formed, which in turn confirmed the presence of the  $CO_3^{2-}$  ion in compound **1**.

**Test 2.** In a 15 mL test tube, 5 mL of a 0.1 mmol solution of compound **1** was treated with 5 mL of 0.1 M hydrochloric acid. An immediate gas effervescence was observed along with the generation of a bright blue-coloured solution. The effervescence confirmed the presence of carbon dioxide in the form of carbonate, and the generation of the bright blue colour in the solution indicated the presence of vanadium in the +4 oxidation state.

### CO<sub>2</sub> exclusion from compound **1** in a gas–solid interface reaction followed by Grignard reaction

2.2 g (1 mmol) of compound **1**, having encapsulated carbonate anion, was taken in a three-neck round-bottom flask and reacted with dry HCl vapours at 5 °C. The generated CO<sub>2</sub> was passed through a dry tetrahydrofuran (THF) solution of trimethylamine to trap the unreacted HCl vapours and allowed to react with 2 mL of freshly prepared 0.1 M PhMgBr reagent in 10 mL of THF at –80 °C. The reaction mixture was mixed with water and the pH was adjusted to 6.3 with 1 M aqueous HCl solution and then extracted with diethyl ether. The resultant reaction mixture was analysed through HRMS to identify the resulting products.

### Manganometric redox titrations of compounds **1** and **2**

Prior to the preparation of solutions, the solvents used were saturated with UHP nitrogen gas to remove dissolved oxygen. 0.05 N potassium permanganate solution (KMnO<sub>4</sub>) was prepared and standardized with 0.05 N ammonium ferrous sulphate ((NH<sub>4</sub>)<sub>2</sub>Fe(SO<sub>4</sub>)<sub>2</sub>·6H<sub>2</sub>O) in 0.2 N sulphuric acid solution. The titrations were carried out completely under nitrogen atmosphere at room temperature to prevent the interaction of air with the vanadium(IV) ion solution. The 0.05 N solution was freshly prepared by dissolving the corresponding vanadium(IV) compound in 0.2 N H<sub>2</sub>SO<sub>4</sub> solution. 10 mL of the above solution was transferred into an Erlenmeyer flask and 0.2 mL of 85% H<sub>3</sub>PO<sub>4</sub> (syrupy phosphoric acid) as catalyst and 2 drops of ferroin as the redox indicator were added. The mixture was titrated against standardized 0.05 N potassium permanganate solution (KMnO<sub>4</sub>). The endpoint was realized by a colour change from red to pale green. The experiment was repeated for two concurrent values. The obtained results and calculations are given in the ESI (section S8†).

### X-ray crystallography

Single crystals of compounds **1** and **2**, suitable to collect diffraction data, were obtained directly from the reaction mixture.

**Table 1** Crystal data and structure refinement parameters for compounds **1** and **2**

	<b>1</b>	<b>2</b>
Empirical formula	CH <sub>88</sub> N <sub>6</sub> Na <sub>6</sub> O <sub>73</sub> V <sub>15</sub>	ClH <sub>63</sub> Na <sub>10</sub> O <sub>66</sub> V <sub>15</sub>
Formula weight	2254.77	2148.93
<i>T</i> (K)/λ (Å)	100(2)/0.71073	293(2)/0.71073
Crystal system	Hexagonal	Hexagonal
Space group	<i>P</i> 6̄2 <i>c</i>	<i>P</i> 6̄2 <i>m</i>
<i>a</i> /Å	12.9910(6)	13.0800(18)
<i>b</i> /Å	12.9910(6)	13.0800(18)
<i>c</i> /Å	23.1099(12)	11.160(2)
α (°)	90	90
β (°)	90	90
γ (°)	120	120
Volume (Å <sup>3</sup> )	3377.5(4)	1635.5(5)
<i>Z</i>	2	1
<i>P</i> calcd (g cm <sup>−3</sup> )	2.130	2.094
μ (mm <sup>−1</sup> ), <i>F</i> (000)	2.140, 2086	2.237, 1000
Goodness-of-fit on <i>F</i> <sup>2</sup>	1.085	1.065
<i>R</i> <sub>1</sub> / <i>wR</i> <sub>2</sub> [ <i>I</i> > 2σ( <i>I</i> )]	0.0285/0.0769	0.0585/0.1753
<i>R</i> <sub>1</sub> / <i>wR</i> <sub>2</sub> (all data)	0.018(6)	0.02(9)
Largest diff. peak/hole (e Å <sup>−3</sup> )	2.384/−0.705	1.005/−0.797

Single-crystal X-ray diffraction data of **1** and **2** were collected at 100 K and 293 K, respectively, on a Bruker Smart Apex III single-crystal X-ray diffractometer equipped with a CCD area detector system, graphite monochromator and a Mo-Kα fine-focus sealed tube (λ = 0.71073 Å). The scans were recorded with a ω scan width of 0.3°. Data reduction was performed using SAINT PLUS,<sup>58</sup> and empirical absorption corrections using equivalent reflections were performed by the program SADABS.<sup>59</sup> Structure solutions were done using SHELXT-2014,<sup>60</sup> and full-matrix least-squares refinement was carried out using SHELXL-2018.<sup>61</sup> All of the non-H atoms were refined anisotropically. Compound **1** crystallizes in the hexagonal *P*6̄2*c* space group and compound **2** crystallizes in the hexagonal *P*6̄2*m* space group. The important crystallographic data of compounds **1** and **2** were given in Table 1. The details of the bond distances and angles corresponding to compounds **1** and **2** were provided in the ESI Tables S1 and S2† containing the supplementary crystallographic data for compounds **1** and **2**; CCDC 1839257† and CSD 434477 contain the supplementary crystallographic data for compounds **1** and **2**, respectively.

## Results and discussion

The synthesis of the deep green-colored compound [Na<sub>6</sub>(H<sub>2</sub>O)<sub>24</sub>][H<sub>8</sub>V<sub>15</sub>O<sub>36</sub>(CO<sub>3</sub>)]·3N<sub>2</sub>H<sub>4</sub>·10H<sub>2</sub>O (**1**) was carried out in an aqueous medium under ambient conditions. The synthesis involves NaVO<sub>3</sub> as the vanadium precursor, N<sub>2</sub>H<sub>5</sub>·HSO<sub>4</sub> as the reducing agent, a small quantity (10 mol%) of α-Bi<sub>2</sub>O<sub>3</sub> and solid NaOH (to adjust the pH to 8.5). Compound **1** (which does not contain any bismuth) cannot be synthesized in absence of α-Bi<sub>2</sub>O<sub>3</sub> from the concerned reaction mixture. It is also important to mention that no external CO<sub>3</sub><sup>2−</sup> source was used for the preparation of **1**, and the spontaneous absorption of atmospheric CO<sub>2</sub> is the only possible source of encapsulated CO<sub>3</sub><sup>2−</sup> in **1**. Thus, α-Bi<sub>2</sub>O<sub>3</sub> plays an important role in the encap-

sulation of dissolved atmospheric CO<sub>2</sub> (in the alkaline aqueous synthesis mixture) into the cavity of the {V<sub>15</sub>} capsule in **1**. It is known that α-Bi<sub>2</sub>O<sub>3</sub> shows a weak synergetic interaction with CO<sub>2</sub> in an alkaline solution.<sup>62–65</sup> Based on this, we speculated that in the present aqueous alkaline synthesis of compound **1**, α-Bi<sub>2</sub>O<sub>3</sub> establishes a reversible equilibrium with absorbed atmospheric CO<sub>2</sub>: α-Bi<sub>2</sub>O<sub>3</sub> + CO<sub>2</sub> ⇌ (BiO)<sub>2</sub>CO<sub>3</sub>, and supplies the carbonate anion to compound **1** for its encapsulation. In order to understand the survival of Bi<sub>2</sub>O<sub>3</sub> in the concerned reaction mixture before and after crystallization, we performed FESEM studies along with elemental mapping on the reaction mixture by analyzing the sample solution after one day and after four days of reaction. (In this synthesis, crystallization begins after two days of reaction.) FESEM images of the reaction mixture collected after one day showed the presence of some flake-shaped particles decorated on sphere-shaped vanadium-containing particles. In the case of reaction mixture collected after four days, FESEM images showed the presence of a similar type of flake-shaped particles, but on needle-shaped vanadium-containing crystals (since the crystallization process had already started). The elemental map of these flake-shaped particles of both instances showed mainly the existence of bismuth and oxygen. Thus, it was determined that the solution contained some amount of bismuth- and oxygen-containing compounds that could be Bi<sub>2</sub>O<sub>3</sub>. The existence of Bi(OH)<sub>3</sub> (in the alkaline reaction mixture) and elemental bismuth (under reducing condition) could not be ruled out (see section S1, ESI† for FESEM images and concerned elemental maps).

The crystal structure of **1** reveals that an encapsulated CO<sub>3</sub><sup>2-</sup> anion was surrounded by 15 vanadium and 21 oxygen atoms spherically in the fully reduced POV capsule anion [H<sub>8</sub>V<sub>15</sub>O<sub>36</sub>(CO<sub>3</sub>)]<sup>6-</sup>. The carbonate anion was stabilized by coordination with three vanadate units {V–O(CO<sub>3</sub><sup>2-</sup>) = 2.30 Å} in the cavity of the POV capsule. The POV cluster displays 12 {VO<sub>5</sub>} square pyramidal units and three distorted octahedral {VO<sub>6</sub>} units that were formed *via* coordination with the central encapsulated CO<sub>3</sub><sup>2-</sup> anion, as shown in Fig. 1. Each of these three vanadium centers, coordinated to the central CO<sub>3</sub><sup>2-</sup>, lie about 0.39 Å above the mean plane of the four equatorial oxygen atoms. On the other hand, in each of twelve VO<sub>5</sub> centers, the vanadium is located about 0.631 Å above the

mean plane of the concerned basal square plane of the four oxygen atoms. This implies that the interactions between peripheral vanadium atoms and the central carbonate ion are strong enough to consider these as coordinate covalent bonds. The overall topology of the POV cluster (compound **1**) is comparable to that of the mixed-valent POV cluster in the compound, Li<sub>7</sub>[V<sub>7</sub><sup>V</sup>V<sub>8</sub><sup>IV</sup>O<sub>36</sub>(CO<sub>3</sub>)] · *ca.* 39H<sub>2</sub>O, reported by Müller and co-workers.<sup>24</sup>

Since we did not supply any source of CO<sub>3</sub><sup>2-</sup> anions (included in the cavity of the {V<sub>15</sub>} capsule in compound **1**) in the concerned reaction mixture and it is the aerial CO<sub>2</sub> dissolved in alkaline reaction mixture that becomes encapsulated in the internal cavity of compound **1**, we characterized the guest carbonate anion using IR and Raman spectral studies along with TGA-MS and TGA-IR studies besides single-crystal X-ray crystallography. The presence of carbonate can be realized by infrared (IR) bands observed at 1468 and 1406 cm<sup>-1</sup> that can be assigned to stretching frequencies of the carbonate ion (Fig. 2a).

The presence of CO<sub>3</sub><sup>2-</sup> was also realized with the help of online coupled TGA-Infrared (Fig. 2b and Fig. S5, ESI†) and TGA-Mass spectral analysis (Fig. 2c and Fig. S7, ESI†). When the temperature of the sample reached 350 °C, CO<sub>2</sub> stretching vibrations at 2295 cm<sup>-1</sup> and 2345 cm<sup>-1</sup> appeared (*i.e.*, the decomposition of CO<sub>3</sub><sup>2-</sup> as CO<sub>2</sub>). The complete disappearance of CO<sub>2</sub> vibrations occurs at around 445 °C. The TGA-Mass spectra were also consistent with the TGA-IR data and showed a mass loss response, corresponding to CO<sub>2</sub> at a similar temperature region (Fig. 2c and Fig. S7, ESI†). The qualitative analysis test for the CO<sub>3</sub><sup>2-</sup> ion was also performed and consistent positive results were obtained (section S5, Fig. S8, ESI†).

Any carbonate salt, upon reacting with a mineral acid, liberates CO<sub>2</sub> gas (CO<sub>3</sub><sup>2-</sup> + 2H<sup>+</sup> → CO<sub>2</sub> + H<sub>2</sub>O), but not always with an acid vapor. Remarkably, the crystals of the compound [Na<sub>6</sub>(H<sub>2</sub>O)<sub>24</sub>][H<sub>8</sub>V<sub>15</sub>O<sub>36</sub>(CO<sub>3</sub>)] · 3N<sub>2</sub>H<sub>4</sub> · 10H<sub>2</sub>O (**1**) (having a carbonate anion per formula unit) underwent gas–solid interface reaction with HCl vapor with the exclusion of CO<sub>3</sub><sup>2-</sup> from the POV capsule as CO<sub>2</sub> gas, resulting in the formation of an amorphous solid (eqn (1)), as confirmed from its PXRD studies (section S6, ESI†).

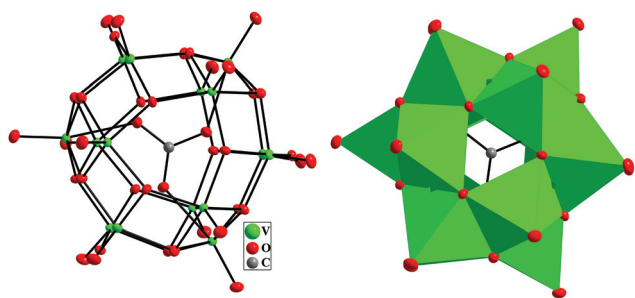
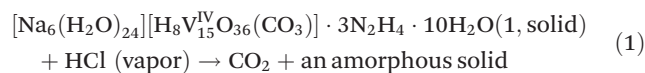


Fig. 1 Thermal ellipsoidal and polyhedral plots (with 60% probability) of the carbonate encapsulated cluster cage, [H<sub>8</sub>V<sub>15</sub>O<sub>36</sub>(CO<sub>3</sub>)]<sup>6-</sup> (compound **1**).

This exclusion of carbonate as CO<sub>2</sub> gas can simply be monitored by IR spectroscopy. The IR bands, observed at 1468 and 1406 cm<sup>-1</sup> for **1**, disappear upon exposing the crystals of **1** to HCl vapor, resulting in the formation of an amorphous substance in a solid-to-solid transformation (eqn (1)). We could not unambiguously characterize the resulting amorphous compound, formed by a gas–solid reaction (eqn (1)). However, ICP-OES elemental analyses of this resulting amorphous solid showed the presence of chlorine. The excluded CO<sub>2</sub> vapor from the encapsulated carbonate, as usually, can be reacted with Grignard reagent, PhMgBr to form triphenylmethanol and benzoic acid (section S7, ESI†) (Scheme 1).

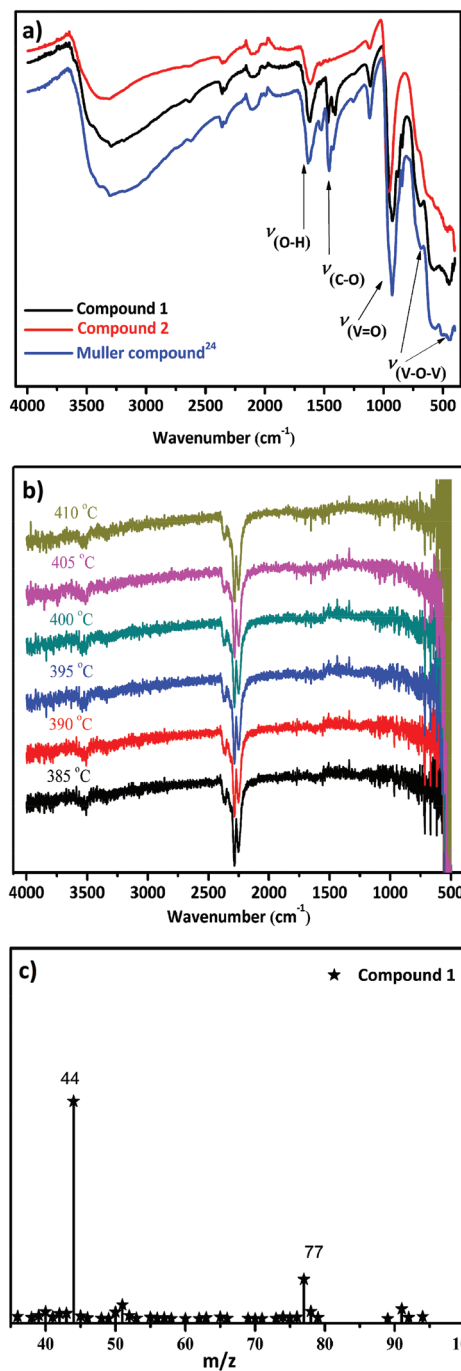
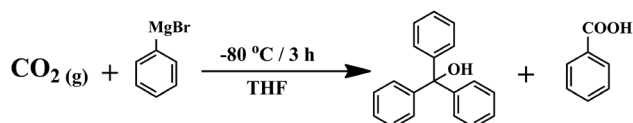


Fig. 2 (a) FTIR spectra of compounds 1, 2 and the Müller mixed-valent compound  $\text{Li}_7[\text{V}_7^{\text{V}}\text{V}_8^{\text{IV}}\text{O}_{36}(\text{CO}_3)] \sim \text{ca.} \cdot 39\text{H}_2\text{O}$ .<sup>24</sup> (prominent carbonate stretching bands of 1 and the Müller mixed-valent compound were located at 1468 and 1406  $\text{cm}^{-1}$ , whereas compound 2 show none of these bands in that region). (b) TGA-IR spectral profile of compound 1 displaying stretching bands corresponding to  $\text{CO}_2$  evolution as a result of  $\text{CO}_3^{2-}$  decomposition in 1. (c) TGA-Mass spectrum of compound 1 displaying a peak corresponding to  $\text{CO}_2$  evolution as a result of  $\text{CO}_3^{2-}$  decomposition in 1.

As we could not unambiguously characterize the amorphous compound formed in the gas–solid reaction (as it loses crystallinity during its solid-to-solid state formation), and it



Scheme 1 Conversion of  $\text{CO}_2$ , excluded from compound 1, to triphenylmethanol and benzoic acid by reacting with  $\text{PhMgBr}$ .

was found to contain chlorine (ICP-OES), we intended to synthesize a chloride anion-encapsulated compound through direct synthesis. Thus, we performed a synthesis similar to the synthesis of compound 1 but added an excess amount of  $\text{NaCl}$  at the end. We indeed isolated and structurally characterized a  $\text{Cl}^-$  ion included compound  $[\text{Na}_{10}(\text{H}_2\text{O})_{24}][\text{H}_3\text{V}_{15}\text{O}_{36}(\text{Cl})] \cdot 6\text{H}_2\text{O}$  (2), in which a chloride anion was found to be encapsulated in the internal cavity of the same  $\{\text{V}_{15}\}$  cluster found in compound 1. The crystal structure of this chloride anion-encapsulated cluster cage is shown in Fig. 3. As far as compositions are concerned, the compound 2 POV cluster anion encapsulates a  $\text{Cl}^-$  in its cavity (Fig. 3) and is tri-protonated in contrast to the compound 1 POV cluster anion, which encapsulates a  $\text{CO}_3^{2-}$  anion in its cavity and is protonated by 8  $\text{H}^+$ . The  $\text{Cl}^-$  ion at the center of the cluster shell (compound 2) does not have any significant interactions with the cluster cage and hence is stabilized by electrostatic interactions.

The presence of the same  $\{\text{V}_{15}\}$  cluster cage in compound 2 can also be established by comparing its Raman signal with that of compound 1. As shown in Fig. 4, the Raman signals of compounds 1, 2 and the known mixed-valent compound  $\text{Li}_7[\text{V}_7^{\text{V}}\text{V}_8^{\text{IV}}\text{O}_{36}(\text{CO}_3)] \sim \text{ca.} \cdot 39\text{H}_2\text{O}$ <sup>24</sup> are comparable. More specifically, the Raman bands corresponding to  $\text{V}-\text{O}(\mu_2\text{-O}/\mu_3\text{-O})$  stretchings, observed for 1 and 2 in the range of 200–650  $\text{cm}^{-1}$ , are comparable to those found for the iso-structural mixed-valent compound  $\text{Li}_7[\text{V}_7^{\text{V}}\text{V}_8^{\text{IV}}\text{O}_{36}(\text{CO}_3)] \sim \text{ca.} \cdot 39\text{H}_2\text{O}$ .<sup>24</sup> The Raman spectral results are consistent with the IR spectral results (Fig. 2a, *vide supra*). Careful analysis shows an extra but small feature at around 800  $\text{cm}^{-1}$  in the Raman spectra of 1 as well as in the mixed-valent compound (both are carbonate anion-containing compounds), which is not present in the Raman spectrum of 2 (chloride anion encapsulated compound 2). We can thus assign this band at around 800  $\text{cm}^{-1}$  in the Raman spectra of both compounds to the Raman active  $A'$  mode of  $\text{D}_3\text{h}$  carbonate.<sup>66</sup>

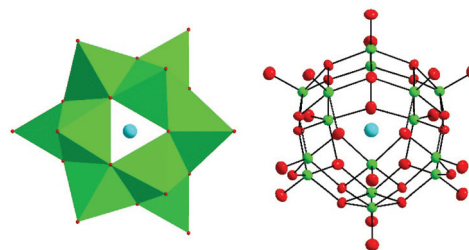


Fig. 3 Polyhedral and thermal ellipsoidal plots (with 60% probability) of the chloride-encapsulated cluster cage,  $[\text{H}_3\text{V}_{15}^{\text{V}}\text{O}_{36}(\text{Cl})]^{10-}$  (in compound 2).

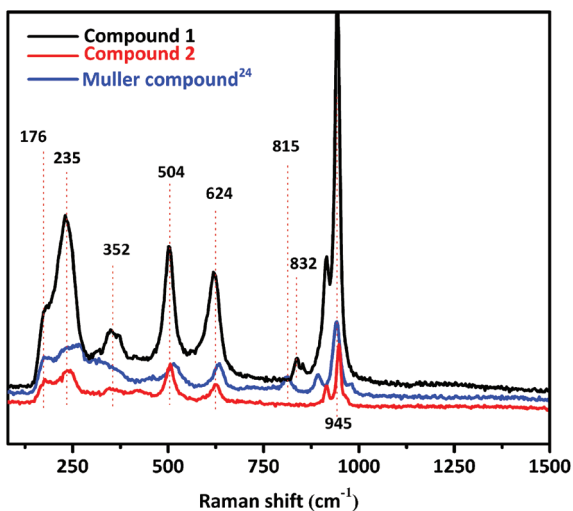


Fig. 4 Raman spectra of compounds 1 and 2 along with the Müller's mixed-valent compound  $\text{Li}_7[\text{V}_7^{\text{V}}\text{V}_8^{\text{IV}}\text{O}_{36}(\text{CO}_3)] \sim \text{ca.} \cdot 39\text{H}_2\text{O}$ .<sup>24</sup>

There are only very few organic-free fully reduced polyoxovanadate (POV) cluster-containing compounds; interestingly, all of them were reported by Müller's group.<sup>13,19,20,47</sup> All these fully reduced organic-free POV compounds were reported to exhibit remarkable magnetism. Compounds 1 and 2 (present work) are new additions to this rare class of organic free fully reduced vanadium-based magnetic materials. Thus, we have recorded magnetic susceptibilities of compounds 1 and 2 at 0.1 T in the temperature range of 3–300 K. Fig. 5 shows the magnetic behaviors of compounds 1 and 2 in the form of  $\chi_M$  versus  $T$  and the product  $\chi_M T$  versus  $T$  plots, respectively. The  $\chi_M T$  value of compound 1 at 300 K is  $5.758 \text{ cm}^3 \text{ K mol}^{-1}$  ( $6.786\mu_B$ ), which is very close to the total spin-only value  $5.626 \text{ cm}^3 \text{ K mol}^{-1}$  ( $6.708\mu_B$ ), expected for 15 non-interacting electrons. In the case of compound 2, the corresponding value is  $4.104 \text{ cm}^3 \text{ K mol}^{-1}$  at 300 K, which is significantly less compared to the total spin-only value ( $6.708\mu_B$ , expected for 15 non-interacting electrons). As shown in Fig. 5, as the temperature decreases, the  $\chi_M T$  value of 1 decreased linearly and reached  $2.36 \text{ cm}^3 \text{ K mol}^{-1}$  at 42 K. The value decreased rapidly below 42 K and reached  $1.104 \text{ cm}^3 \text{ K mol}^{-1}$  at 3 K. This behaviour does not follow Curie and Curie–Weiss law and seems to be the antiferromagnetic interactions of individual spins in 1. On the other hand, the  $\chi_M T$  value of 2 is constant when the temperature is varied from 300 K to 250 K, but decreased linearly to  $0.39 \text{ cm}^3 \text{ K mol}^{-1}$  with the decrease of temperature from 250 K to 3 K. The  $\chi_M T$  value of  $0.39 \text{ cm}^3 \text{ K mol}^{-1}$  at 3 K for 2 is close to zero and infers an  $S = 0$  ground state for 2. Thus, the magnetic susceptibilities of 1 as a function of temperature are considerably different from 2 as a function of temperature. This clearly suggests that the encapsulated and coordinated carbonate anion in 1 as the guest facilitates a different magnetic pathway compared to the magnetic exchange pathways, shown by compound 2 having non-coordinated encapsulated  $\text{Cl}^-$  anions as the guest. However, the

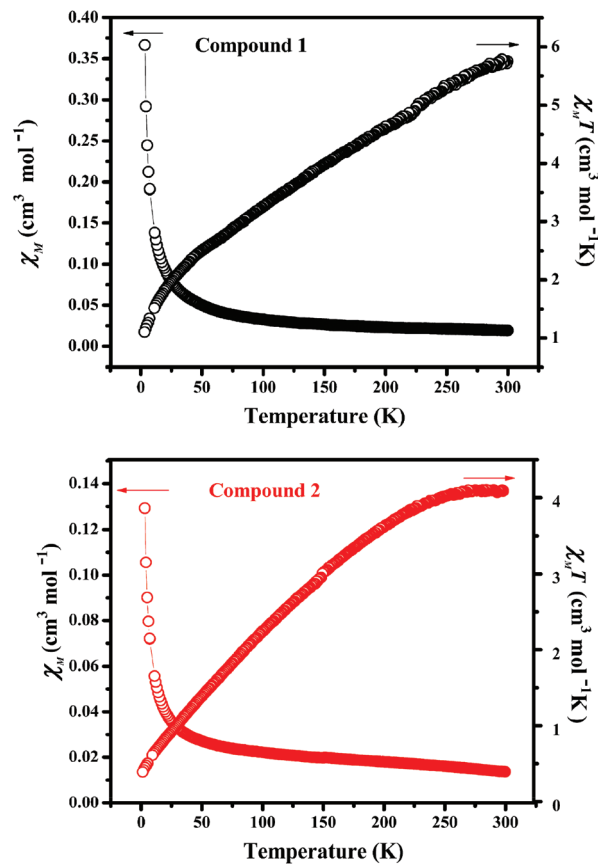


Fig. 5  $\chi_M$  vs.  $T$  and  $\chi_M T$  vs.  $T$  plots of compounds 1 and 2: temperature dependences of  $\chi_M$  and  $\chi_M T$ .

detailed account of magnetic interactions, including theoretical studies, in compounds 1 and 2 are not possible at this stage and will be reported later in detail.

The bond valence sum calculations conclude that, all vanadium centers in 1 and 2 are in the +4 oxidation state in contrast to the vanadium centers of same cluster cage containing the compound  $\text{Li}_7[\text{V}_7^{\text{V}}\text{V}_8^{\text{IV}}\text{O}_{36}(\text{CO}_3)] \sim \text{ca.} \cdot 39\text{H}_2\text{O}$  (mixed-valent compound),<sup>24</sup> which has 7 vanadium atoms in the +5 oxidation state and 8 vanadium atoms in the +4 oxidation state. Accordingly, the bond distances around the vanadium centres in 1 and 2 are quite different from those in  $\text{Li}_7[\text{V}_7^{\text{V}}\text{V}_8^{\text{IV}}\text{O}_{36}(\text{CO}_3)] \sim \text{ca.} \cdot 39\text{H}_2\text{O}$ <sup>24</sup> and other mixed-valent  $\{\text{V}_{18}\text{O}_{42}\}$  systems.<sup>40</sup> The bond valence sum calculations (BVS) on 1 and 2 (section S8, ESI†) furnishes that the relevant BVS values are in the ranges of 3.40–4.22 (Avg. = 3.89) and 3.87–4.28 (Avg. = 4.11) for 1 and 2, respectively. The average V–O terminal bond distances (1.62–1.64) are significantly longer in 1 and 2 compared to the same distances reported for mixed-valent and fully oxidized polyoxovanadates.<sup>67</sup> This observation is also consistent with the +4 oxidation state of the vanadium centers in 1 and 2. In order to support the BVS calculations, we recorded the X-ray photoelectron spectra (XPS) of compounds 1 and 2, whereby O 1s response at 530 eV was taken as the reference. Fig. 6 (see also, section S9, ESI†) shows the partial XPS plots of 1 and 2. Both compounds display a signal

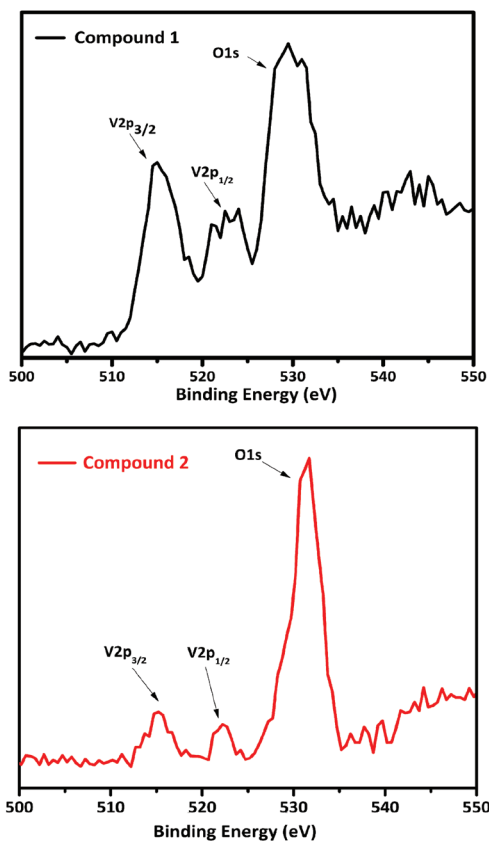


Fig. 6 Core level X-ray photoelectron spectroscopy of compounds 1 and 2.

in the range of 514.96–515.73 eV for V  $2p_{3/2}$  with FWHM (full width at half maximum) of 2.73–4.27 eV, which is characteristic for the vanadium(IV) oxidation state.<sup>68</sup> Another XPS signal with relatively weak intensity was also observed in the range of 522.50–523.12 eV corresponding to V  $2p_{1/2}$ . The volumetric redox titrations of nitrogen gas purged aqueous solutions of 1 and 2 using standardized  $\text{KMnO}_4$  solution, and ferrion as an indicator also revealed the presence of 15 electrons per formula unit of each compound, 1 and 2 (section S10, ESI†).

Apart from the above-mentioned BVS, XPS, and volumetric redox titration confirmations, the presence of the V (IV) oxidation states of 1 and 2 can be realized with the help of d–d transitions in their UV-Vis spectra. For this, 0.1 M  $\text{lit}^{-1}$  aqueous solutions (based on the  $\text{V}^{4+}$  metal ion, 0.1 M per mL) of compounds 1 and 2 were used to record UV-vis absorption (solution) spectra. The d–d transitions corresponding to  $\text{V}^{4+}$  ( $d^1$ ) ion in the region of 600 to 1200 nm with an absorption maxima at 964 nm for 1 and at 995 nm for 2 (Fig. 7) were observed.<sup>69,70</sup> The bands below 400 nm are perhaps due to ligand-to-metal charge transfer ‘LM-CT’ ( $\text{O} \rightarrow \text{V}$ ) transitions.

The thermal stability of the compounds 1 and 2 was examined by TGA analysis under helium gas atmosphere (Fig. 8). The TGA analysis revealed that compound 1 shows two-stage dissociation of lattice water and hydrazine molecules as well as sodium coordinated water molecules, followed by  $\text{CO}_2$  evolution

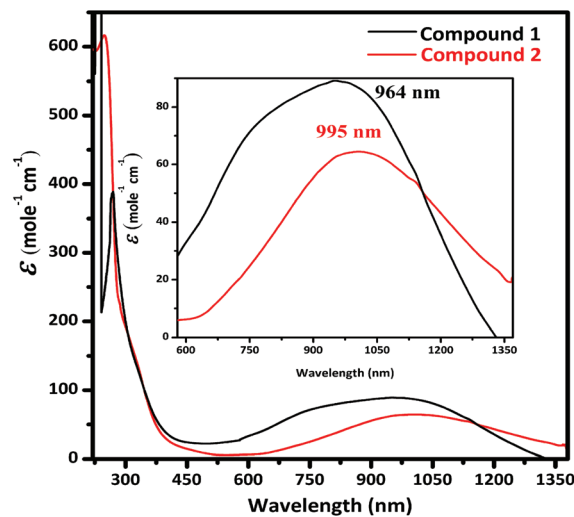


Fig. 7 UV-Vis absorption (solution) spectra of 1 and 2 in water.

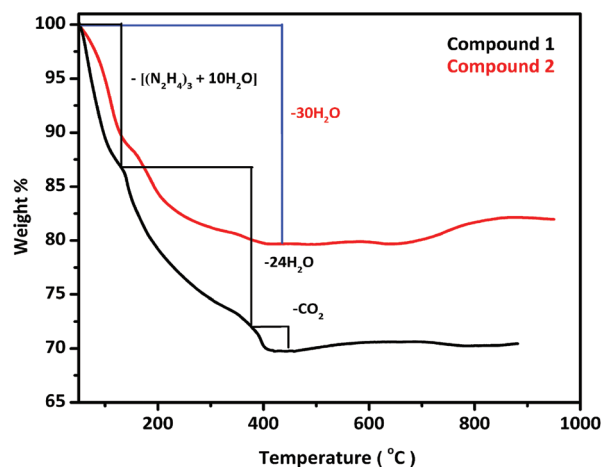


Fig. 8 Thermogravimetric analyses plots of compounds 1 and 2.

with the decomposition of the  $\text{CO}_3^{2-}$  ion. However, the cluster showed much thermal stability up to 495 °C and then decomposes. In contrast, compound 2 showed gradual weight loss in the temperature range of 50 to 400 °C, corresponding to the water of crystallization and remained stable up to 600 °C.

## Conclusions

In conclusion, even though it is known that an alkaline aqueous solution absorbs aerial  $\text{CO}_2$  gas and that aqueous polyoxometalate chemistry had long been known (for over 200 years), not a single polyoxometalate compound had been reported until today, in which the absorbed aerial  $\text{CO}_2$  was encapsulated. We made this inclusion (as the carbonate) possible by using some amount of  $\alpha\text{-Bi}_2\text{O}_3$  in the relevant reaction mixture. We characterized this confined carbonate anion by IR, TGA-Mass, and TGA-IR spectral studies including single-crystal X-ray crystallography. We have to admit that even

though the terminal source of this carbonate encapsulation is air, this will not solve the global warming problem (as one big cluster anion encapsulates only one carbonate anion). However, the present host-guest system is unique in the sense that this, upon exposure to HCl vapor, excludes the guest carbonate anion as CO<sub>2</sub> gas leading to the formation of an amorphous material. The excluded CO<sub>2</sub> can react with PhMgBr (a Grignard reagent) to produce useful organic products (triphenylcarbinol and benzoic acid). We could not characterize the resulting amorphous material (formed after CO<sub>2</sub> exclusion with HCl vapor in a solid-to-solid transformation). Elemental analysis of this amorphous material showed the presence of not only the chlorine element but also a good amount of hydrogen content even after thorough washing with water. A preliminary measurement on this amorphous material showed that it exhibits excellent proton conduction in the solid state. Detailed studies in this direction are under way.

## Author contributions

The manuscript was written through the contributions of all authors. All authors have given approval to the final version of the manuscript.

## Conflicts of interest

The authors declare no competing financial interests.

## Acknowledgements

The authors thank SERB, DST, Government of India (Project No. EMR/2017/002971) for their financial support. S. Mulkapuri thanks, UGC, New Delhi, India, for the fellowship and S. K. Kurapati thanks the UGC, New Delhi, India for awarding the Dr D. S. Kothari Post-Doctoral Fellowship (Award Letter No. F.4-2/2006 (BSR)/CH/15-16/0074). We also thank DST-FIST, UGC-SAP, and UPE-II.

## References

- 1 D. E. Katsoulis, *Chem. Rev.*, 1998, **98**, 359–388.
- 2 W.-H. Fang, L. Zhang and J. Zhang, *Chem. Soc. Rev.*, 2018, **47**, 404–421.
- 3 N. V. Izarova, M. T. Pope and U. Kortz, *Angew. Chem., Int. Ed.*, 2012, **51**, 9492–9510.
- 4 S.-S. Wang and G.-Y. Yang, *Chem. Rev.*, 2015, **115**, 4893–4962.
- 5 H. Lv, Y. V. Geletii, C. Zhao, J. W. Vickers, G. Zhu, Z. Luo, J. Song, T. Lian, D. G. Musaev and C. L. Hill, *Chem. Soc. Rev.*, 2012, **41**, 7572–7589.
- 6 D.-L. Long, E. Burkholder and L. Cronin, *Chem. Soc. Rev.*, 2007, **36**, 105–121.
- 7 N. I. Gumerova and A. Rompel, *Nat. Rev. Chem.*, 2018, **2**, 0112.
- 8 A. Fernando, K. L. D. M. Weerawardene, N. V. Karimova and C. M. Aikens, *Chem. Rev.*, 2015, **115**, 6112–6216.
- 9 H. N. Miras, J. Yan, D.-L. Long and L. Cronin, *Chem. Soc. Rev.*, 2012, **41**, 7403–7430.
- 10 J. J. Chen, M. D. Symes, S. C. Fan, M. S. Zheng, H. N. Miras, Q. F. Dong and L. Cronin, *Adv. Mater.*, 2015, **27**, 4649–4654.
- 11 J. J. Chen, J. C. Ye, X. G. Zhang, M. D. Symes, S. C. Fan, D. L. Long, M. S. Zheng, D. Y. Wu, L. Cronin and Q. F. Dong, *Adv. Energy Mater.*, 2017, **8**, 1701021.
- 12 J. T. Rhule, C. L. Hill, D. A. Judd and R. F. Schinazi, *Chem. Rev.*, 1998, **98**, 327–358.
- 13 A. Müller, F. Peters, M. T. Pope and D. Gatteschi, *Chem. Rev.*, 1998, **98**, 239–272.
- 14 K. Y. Monakhov, W. Bensch and P. Kogerler, *Chem. Soc. Rev.*, 2015, **44**, 8443–8483.
- 15 R. E. P. Winpenny, *Adv. Inorg. Chem.*, 2001, **52**, 1–11.
- 16 A. Barbour, R. D. Luttrell, J. Choi, J. L. Musfeldt, D. Zipse, N. S. Dalal, D. W. Boukhvalov, V. V. Dobrovitski, M. I. Katsnelson, A. I. Lichtenstein, B. N. Harmon and P. Kögerler, *Phys. Rev. B: Condens. Matter Mater. Phys.*, 2006, **74**, 014411.
- 17 I. Chiorescu, W. Wernsdorfer, A. Müller, H. Bögge and B. Barbara, *J. Magn. Magn. Mater.*, 2000, **221**, 103–109.
- 18 K. Hegetschweiler, B. Morgenstern, J. Zubieta, P. J. Hagerman, N. Lima, R. Sessoli and F. Totti, *Angew. Chem., Int. Ed.*, 2004, **43**, 3432–3436.
- 19 D. Gatteschi, L. Pardi, A. L. Barra, A. Müller and J. Döring, *Nature*, 1991, **354**, 463–465.
- 20 A.-L. Barra, D. Gatteschi, L. Pardi, A. Müller and J. Döring, *J. Am. Chem. Soc.*, 1992, **114**, 8509–8514.
- 21 P. Yang, M. Alsufyani, A.-H. Emwas, C. Chen and N. M. Khashab, *Angew. Chem., Int. Ed.*, 2018, **57**, 13046–13051.
- 22 A. Müller, S. K. Das, P. Kögerler, H. Bögge, M. Schmidtman, A. X. Trautwein, V. Schünemann, E. Krickemeyer and W. Preetz, *Angew. Chem., Int. Ed.*, 2000, **39**, 3413–3417.
- 23 A. Müller, H. Reuter and S. Dillinger, *Angew. Chem., Int. Ed. Engl.*, 1995, **34**, 2328–2361.
- 24 A. Müller, M. Penk, R. Rohlfing, E. Krickemeyer and J. Döring, *Angew. Chem., Int. Ed. Engl.*, 1990, **29**, 926–927.
- 25 T. Yamase and K. Ohtaka, *J. Chem. Soc., Dalton Trans.*, 1994, 2599–2608.
- 26 V. W. Day, W. G. Klemperer and O. M. Yaghi, *J. Am. Chem. Soc.*, 1989, **111**, 5959–5961.
- 27 A. Müller, R. Rohlfing, E. Krickemeyer and H. Bögge, *Angew. Chem., Int. Ed. Engl.*, 1993, **32**, 909–912.
- 28 N. Watfa, D. Melgar, M. Haouas, F. Taulelle, A. Hijazi, D. Naoufal, J. B. Avalos, S. Floquet, C. Bo and E. Cadot, *J. Am. Chem. Soc.*, 2015, **137**, 5845–5851.
- 29 M. A. Moussawi, N. Leclerc-Laronze, S. Floquet, P. A. Abramov, M. N. Sokolov, S. Cordier, A. Ponchel, E. Monflier, H. Bricout, D. Landy, M. Haouas, J. Marrot and E. Cadot, *J. Am. Chem. Soc.*, 2017, **139**, 12793–12803.
- 30 Y. Kikukawa, K. Seto, S. Uchida, S. Kuwajima and Y. Hayashi, *Angew. Chem., Int. Ed.*, 2018, **57**, 16051–16055.

- 31 N. Kawanami, T. Ozeki and A. Yagasaki, *J. Am. Chem. Soc.*, 2000, **122**, 1239–1240.
- 32 S. Kuwajima, Y. Kikukawa and Y. Hayashi, *Chem. – Asian J.*, 2017, **12**, 1909–1914.
- 33 Y. Inoue, Y. Kikukawa, S. Kuwajima and Y. Hayashi, *Dalton Trans.*, 2016, **45**, 7563–7569.
- 34 S. Kuwajima, Y. Ikinobu, D. Watanabe, Y. Kikukawa, Y. Hayashi and A. Yagasaki, *ACS Omega*, 2017, **2**, 268–275.
- 35 A. Müller, E. Krickemeyer, M. Penk, H.-J. Walberg and H. Bögge, *Angew. Chem., Int. Ed. Engl.*, 1987, **26**, 1045–1046.
- 36 B. Dong, J. Peng, Y. Chen, Y. Kong, A. Tian, H. Liu and J. Sha, *J. Mol. Struct.*, 2006, **788**, 200–205.
- 37 C.-D. Zhang, S.-X. Liu, B. Gao, C.-Y. Sun, L.-H. Xie, M. Yu and J. Peng, *Polyhedron*, 2007, **26**, 1514–1522.
- 38 Y. Chen, J. Peng, H. Yu, Z. Han, X. Gu, Z. Shi, E. Wang and N. Hu, *Inorg. Chim. Acta*, 2005, **358**, 403–408.
- 39 B.-x. Dong, J. Peng, C. J. Gómez-García, S. Benmansour, H.-q. Jia and N.-h. Hu, *Inorg. Chem.*, 2007, **46**, 5933–5941.
- 40 Y.-l. Teng, B.-X. Dong, J. Peng, S.-Y. Zhang, L. Chen, L. Song and J. Ge, *CrystEngComm*, 2013, **15**, 2783–2785.
- 41 Y. Chen, X. Gu, J. Peng, Z. Shi, H. Yu, E. Wang and N. Hu, *Inorg. Chem. Commun.*, 2004, **7**, 705–707.
- 42 M. I. Khan, S. Ayesh, R. J. Doedens, M. Yu and C. J. O'Connor, *Chem. Commun.*, 2005, 4658–4660.
- 43 N. Kato and Y. Hayashi, *Dalton Trans.*, 2013, **42**, 11804–11811.
- 44 T. D. Keene, D. M. D'Alessandro, K. W. Krämer, J. R. Price, D. J. Price, S. Decurtins and C. J. Kepert, *Inorg. Chem.*, 2012, **51**, 9192–9199.
- 45 L.-N. Xiao, J.-N. Xu, Y.-Y. Hu, L.-M. Wang, Y. Wang, H. Ding, X.-B. Cui and J.-Q. Xu, *Dalton Trans.*, 2013, **42**, 5247–5251.
- 46 A. Müller, E. Krickemeyer, M. Penk, R. Rohlffing, A. Armatage and H. Bögge, *Angew. Chem., Int. Ed. Engl.*, 1991, **30**, 1674–1677 and references therein.
- 47 A. Müller, R. Sessoli, E. Krickemeyer, H. Bögge, J. Meyer, D. Gatteschi, L. Pardi, J. Westphal, K. Hovemeier, R. Rohlffing, J. Döring, F. Hellweg, C. Beugholt and M. Schmidtman, *Inorg. Chem.*, 1997, **36**, 5239–5250.
- 48 M. I. Khan, E. Yohannes and R. J. Doedens, *Angew. Chem., Int. Ed.*, 1999, **38**, 1292–1294.
- 49 T. Yamase, M. Suzuki and K. Ohtaka, *J. Chem. Soc., Dalton Trans.*, 1997, 2463–2472.
- 50 *Climate Change 2007: Synthesis Report, International Panel on Climate Change*, Cambridge University Press, Cambridge, UK, 2007.
- 51 P. Falkowski, R. J. Scholes, E. Boyle, J. Canadell, D. Canfield, J. Elser, N. Gruber, K. Hibbard, P. Höglberg, S. Linder, F. T. Mackenzie, B. Moore III, T. Pedersen, Y. Rosenthal, S. Seitzinger, V. Smetacek and W. Steffen, *Science*, 2000, **290**, 291.
- 52 B. Yu, B. Zou and C.-W. Hu, *J. CO<sub>2</sub> Util.*, 2018, **26**, 314–322 and references therein.
- 53 S. Garai, E. T. K. Haupt, H. Bögge, A. Merca and A. Müller, *Angew. Chem., Int. Ed.*, 2012, **51**, 10528–10531.
- 54 G. Gao, F. Li, L. Xu, X. Liu and Y. Yang, *J. Am. Chem. Soc.*, 2008, **130**, 10838–10839.
- 55 A. M. Khenkin, I. Efremenko, L. Weiner, J. M. L. Martin and R. Neumann, *Chem. – Eur. J.*, 2010, **16**, 1356–1364.
- 56 N. E. Levinger, L. C. Rubenstrunk, B. Baruah and D. C. Crans, *J. Am. Chem. Soc.*, 2011, **133**, 7205–7214.
- 57 W. Cheng, Y.-s. Xue, X.-M. Luo and Y. Xu, *Chem. Commun.*, 2018, **54**, 12808–12811.
- 58 *SAINT: Software for the CCD Detector System*, Bruker Analytical X-ray Systems, Inc., Madison, WI, 1998.
- 59 G. M. Sheldrick, *SADABS, Program for Area Detector Absorption Correction*, University of Gottingen, Gottingen, Germany, 1997.
- 60 G. M. Sheldrick, *Acta Crystallogr., Sect. A: Found. Adv.*, 2015, **71**, 3–8.
- 61 G. M. Sheldrick, *Acta Crystallogr., Sect. C: Struct. Chem.*, 2015, **71**, 3–8.
- 62 P. Taylor, S. Sunder and V. J. Lopata, *Can. J. Chem.*, 1984, **62**, 2863–2873.
- 63 T. Esaka and K. Moto-ike, *Mater. Res. Bull.*, 2004, **39**, 1581–1587.
- 64 M. Nolan, *CO<sub>2</sub> Activation on Heterostructures of Bi<sub>2</sub>O<sub>3</sub>-nanocluster Modified TiO<sub>2</sub>: Promoting the Critical First Step in CO<sub>2</sub> Conversion*, 2018, DOI: 10.26434/chemrxiv.5917351.v1.
- 65 S.-F. Yin, J. Maruyama, T. Yamashita and S. Shimada, *Angew. Chem., Int. Ed.*, 2008, **47**, 6590–6593.
- 66 A. M. Greenaway, T. P. Dasgupta, K. C. Koshy and G. G. Sadler, *Spectrochim. Acta*, 1986, **42**, 949–954.
- 67 W. L. Queen, J. P. West, J. Hudson and S.-J. Hwu, *Inorg. Chem.*, 2011, **50**, 11064–11068.
- 68 G. Silversmit, D. Depla, H. Poelman, G. B. Marin and R. De Gryse, *J. Electron Spectrosc. Relat. Phenom.*, 2004, **135**, 167–175.
- 69 M. Yuan, Y. Li, E. Wang, C. Tian, L. Wang, C. Hu, N. Hu and H. Jia, *Inorg. Chem.*, 2003, **42**, 3670.
- 70 T. Arumuganathan and S. K. Das, *Inorg. Chem.*, 2009, **48**, 496–507.